Performance of Combined PCM/Metal Foam-based Photovoltaic Thermal (PVT) Collector

Mojtaba Dayer[1] (iD), Ag Sufiyan Abd Hamid[2‡] (iD), Kamaruzzaman Sopian[1] (iD), Adnan Ibrahim[1‡] (iD), Anwer. B. Al-Aasam[1] (iD), Bassam Abdulsahib[1,3] (iD), Saeed Rahmanian[4] (iD)

[1] Solar Energy Research Institute, Universiti Kebangsaan Malaysia, Bangi, Selangor, 43600 Malaysia

[2] Faculty of Science and Natural Resources, Kota Kinabalu, Sabah, 88400 Malaysia

[3] Al-Awsat Technical University, 31001 Iraq

[4] Department of Mechanical engineering, Jahrom University, Jahrom, Iran

(dayer.mojtaba@gmail.com, pian@ums.edu.my, ksopian@ukm.edu.my, iadnan@ukm.edu.my, anwor.bassim@gmail.com, p103204@siswa.ukm.edu.my, s.rahmanian@jahromu.ac.ir)

‡Corresponding Authors; pian@ums.edu.my, iadnan@ukm.edu.my

Abstract- Photovoltaic thermal collector (PVT) is a power generation technology that adapts solar radiation into electrical and thermal energy. There are two cooling methods in PV panels: active and passive. Phase Change Materials (PCM) have high latent heat during charging and discharging, making them promising as thermal energy storage. However, their low thermal conductivity remains a major drawback, which was to be solved by porous metal foams given their high thermal conductivity, low density, and lightness. This study aimed to introduce and analyze a novel PVT design by integrating PCM with Copper Foam Matrix (CFM) as passive cooling combined with submerged serpentine copper tubes for fluid flow as active cooling. This novel PVT was run with and without CFM by conducting a 3D steady-state simulation using COMSOL Multiphysics. This study showed that incorporating the PCM plus CFM will decrease the PV surface temperature and increase electrical efficiency. The effective thermal conductivity of PCM increased, leading to higher thermal extraction at the tested mass flow rates. At an irradiance of 1000W/m2 and an ambient temperature of 20°C, the collector achieved 65% and 13% thermal and electrical efficiency, respectively.

Keywords Photovoltaic thermal collector; Phase Change Materials; Metal-foams; Thermal efficiency; Electrical efficiency.

1. Introduction

The working fluid and collector configurations are the two most essential factors in categorizing PVT systems. Some designs may employ water, air, a combination of water and air, or nanofluids as working fluids. Different types of collectors can be distinguished, for instance, by the presence of a tube, heat pipe, and various sheet configurations [1-5]. Tripanagnostopoulos et al. found that glazing has huge effects on the whole system. The finding implies that the collector's cell cover is one of the PVT collector's classifying factors [6].

Due to its minimal complexity and initial expense, air-based PVTs are the most used configuration [7, 8]. However, using liquids as circulating fluids increases the thermal capacitance of systems, resulting in improved cooling [9]. Kazanci et al. examined an application of PCM in a photovoltaic thermal (PVT) system providing heating and cooling for a plus-energy home. Their findings indicated that the PVT efficiency was around 42.8%, while the conventional PV efficiency was 13.59% [10]. Qiu et al. studied the energy of a novel PVT design using Microencapsulated Phase Change Material slurry (MPCM). According to their findings, the greatest electrical efficiency was 8.7%, while the maximum thermal efficiency was 59% [11]. Hassan et al. analyzed a solid-liquid PCM's electrical and thermal energy efficiency with PV panels in two climatic regions. According to their findings, the average efficiencies achieved under the climatic conditions of Pakistan and Ireland were 20.3% and 14.6%, respectively [12]. Fiorentini et al. investigated a novel air-based photovoltaic thermal (PVT) collector with a PCM storage unit and a reverse cycle heat pump for HVAC

applications obtaining 45% thermal and 9% electrical efficiency [13].

Much research has been done to increase the low thermal conductivity of the PCM, which is one of its main drawbacks. Tao et al. evaluated the heat transfer of a porous medium filled with phase change materials by adopting the Lattice Boltzmann method [14]. Tao et al. evaluated the heat transfer of a porous medium filled with phase change materials by adopting the Lattice Boltzmann method [15]. Zhou and Zhao studied on heat transfer of phase change material in a metal foam using the phase-field method [16]. Others proposed a two-temperature model for assessing the performance of PCM-filled metallic foam. They used Darcy-Brinkman equations to shed light on the effect of metal foam [1]. This study increased the PVT module's overall efficiency using water and metal-foam Phase Change Materials (PCM). This research was conducted to improve the collector's overall performance and create a new design for the PVT market.

2. METHODS

2.1. Physical Model

Fig. 1 shows the cross-sectional drawing of the proposed PVT collector and illustrates the different layers of the PVT collector. Comparing the proposed system to a reference system is essential to comprehend its performance. The systems employed are (i) conventional PVT with PCM only, including water flowing to extract the heat, and (ii) a novel proposed system with PCM embedded in copper foam with water flowing. Such a comparison would show how well the collector works when copper foam and PCM are used. To this end, they used porous aluminium (0.8) and paraffin as porous medium and phase change materials, respectively [17].
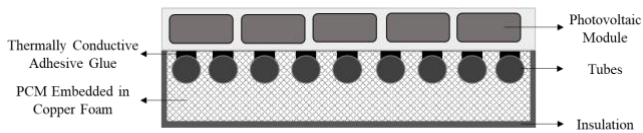

Fig. 1. Cross-sectional drawing of the metal-foam PCM and water-based PVT collector

2.2. Assumptions

The problem was solved by assuming Local Thermal Non-Equilibrium (LTNE) between copper foam and Phase Change Material (PCM). The Brinkmann-Forchheimer extended Darcy equation is used to calculate PCM velocity under incompressibility, the Boussinesq assumption, and the absence of micro inertial effects (Eqs. 1 and 2). It is assumed that the flowing water is laminar and incompressible. For the boundary conditions, all walls are considered to have zero velocity. Heat flux enters the panel from the top. This study splits the heat flux into two parallel PCM and copper foam based on porosity weight.

$$q_{PCM} = q_{fe} = \varepsilon q_{inc} \tag{1}$$

$$q_{CFM} = q_{se} = (1 - \varepsilon)q_{in} \tag{2}$$

Since the effective thermal conductivity of two phases is roughly on the same magnitude scale, it is reasonable to include this assumption. Consequently, the heat flux may be divided according to porosity and boundary condition scaling [18].

2.3. Mathematical Formulation

For heat transfer analysis, the applied governing equations for the water fluid, encompassing mass, momentum, and energy, are as Eqs. 3-5:

$$\frac{\partial \rho_w}{\partial t} + \nabla.(\rho_w V_w) = 0 \tag{3}$$

$$\rho_w \left[\frac{\partial V_w}{\partial t} + (\partial V_w . \nabla)V_w \right] = \nabla P + \nabla.(\mu_w \nabla V_w) \tag{4}$$

$$\rho_w C_{p,w} \frac{\partial T_w}{\partial t} + \rho_w C_{p,w} V_w . \nabla T_w = \nabla.(k_w \nabla T_w) \tag{5}$$

Subscript f denotes heat transfer in fluid, and P, V, ρ, and μ are fluid pressure, velocity vector, density, and dynamic viscosity, respectively. In this 3D modelling with coordinates (x, y, z) and unit vectors of axes $\{\overrightarrow{e_x}, \overrightarrow{e_y}, \overrightarrow{e_z}\}$, ∇ is defined in Eq. 6:

$$\nabla = \overrightarrow{e_x} \frac{\partial}{\partial x} + \overrightarrow{e_y} \frac{\partial}{\partial y} + \overrightarrow{e_z} \frac{\partial}{\partial z} = \left(\frac{\partial}{\partial x}, \frac{\partial}{\partial y}, \frac{\partial}{\partial z} \right) \tag{6}$$

There are two approaches to solving heat transfer between copper foam and PCM: Local Thermal Equilibrium and non-Equilibrium. In this case, the latter is implemented. Local Thermal Non-Equilibrium (LTNE) is a more accurate method to simulate the heat transfer since the thermal conductivity difference between the two regions is significant. The continuity, momentum, and energy equations for the PCM embedded in the copper foam domain are derived as mentioned in Eqs. 7-12:

$$\frac{\partial \rho_f}{\partial t} + \frac{\partial(\rho_f u_f)}{\partial x} + \frac{\partial(\rho_f v_f)}{\partial y} + \frac{\partial(\rho_f w_f)}{\partial z} = 0 \tag{7}$$

$$\frac{\rho_f}{\varepsilon} \frac{\partial u_f}{\partial t} + \frac{\rho_f}{\varepsilon^2} (\overrightarrow{V}\overrightarrow{V}).u_f = -\frac{\partial P_f}{\partial x} + \frac{\mu_f}{\varepsilon} \nabla^2 u_f - \left(\frac{\mu_f}{K} + \frac{\rho_f C_{p,f}}{\sqrt{K}} |u_f| \right) u_f + S_u \tag{8}$$

$$\frac{\rho_f}{\varepsilon} \frac{\partial v_f}{\partial t} + \frac{\rho_f}{\varepsilon^2} (\overrightarrow{V}\overrightarrow{V}).v_f = -\frac{\partial P_f}{\partial y} + \frac{\mu_f}{\varepsilon} \nabla^2 v_f - \left(\frac{\mu_f}{K} + \frac{\rho_f C_{p,f}}{\sqrt{K}} |v_f| \right) v_f + S_v \tag{9}$$

$$\frac{\rho_f}{\varepsilon} \frac{\partial w_f}{\partial t} + \frac{\rho_f}{\varepsilon^2} (\overrightarrow{V}\overrightarrow{V}).w_f = -\frac{\partial P_f}{\partial z} + \frac{\mu_f}{\varepsilon} \nabla^2 w_f - \left(\frac{\mu_f}{K} + \frac{\rho_f C_{p,f}}{\sqrt{K}} |w_f| \right) w_f + S_w + \rho_f g\beta[T_f - (T_m - \Delta T_m)] \tag{10}$$

$$\rho_f c_{p,f} \left(\varepsilon \frac{\partial T_f}{\partial t} + U.\nabla T_f \right) = k_{fe} \nabla^2 T_f + h_{sf} a_{sf} (T_s - T_f) \tag{11}$$

$$(1 - \varepsilon)\rho_s c_{p,s} \frac{\partial T_s}{\partial t} = k_{se} \nabla^2 T_s + h_{sf} a_{sf} (T_f - T_s) \tag{12}$$

The last term in the z-coordinate of the momentum equation is the expression of the Forchheimer extended Darcy model, which demonstrates the non-Darcy and inertia effects incurred by copper foam. The physical parameters of the copper foam structure, expressed in Eqs. 13 - 18:

$$K = \frac{\varepsilon^2}{36\chi(\chi-1)} d_k{}^2 \tag{13}$$

$$\chi = 2 + 2\cos\left[\frac{4\pi}{3} + \frac{1}{3\cos(2\varepsilon - 1)}\right] \qquad (14)$$

$$d_k = \frac{\chi d_p}{(3-\chi)} \qquad (15)$$

$$d_p = \frac{22.4 \times 10^{-3}}{\omega} \qquad (16)$$

$$C = 0.00212(1-\varepsilon)^{-0.132}\left(\frac{d_f}{d_p}\right)^{-1.63} \qquad (17)$$

$$d_f = 1.18\sqrt{\frac{1-\varepsilon}{3\pi}}\,d_p \qquad (18)$$

K, χ, C, d_f, d_p, d_k, ε and ω are the permeability, tortuosity coefficient, inertial coefficient, fibre diameter, pore size, characteristic length, porosity, and pores per inch of copper foam, respectively. The tetrakaidecahedron cell model presented by Boomsma and Poulikakos to represent the effectiveness of thermal conductivity was shown in Eqs. 19 - 26 [19].

$$k_{fe} = k_{eff}|k_s = 0 \qquad (19)$$

$$k_{se} = k_{eff}|k_f = 0 \qquad (20)$$

$$k_{eff} = \frac{\sqrt{2}}{2(R_A + R_B + R_C + R_D)} \qquad (21)$$

$$R_A = \frac{4d}{(2e^2\pi d(1-e))k_s + (4 - 2e^2 - \pi d(1-e))k_f} \qquad (22)$$

$$R_B = \frac{(e-2d)^2}{(e-2d)e^2 k_s + (2e - 4d - (e-2d)e^2)k_f} \qquad (23)$$

$$R_C = \frac{(\sqrt{2}-2e)^2}{2\pi d^2(1-2e\sqrt{2})k_s + 2(\sqrt{2}-2e-\pi d^2(1-e\sqrt{2}))k_f} \qquad (24)$$

$$R_D = \frac{2e}{e^2 k_s + (4-e^2)k_f} \qquad (25)$$

$$d = \sqrt{\frac{\sqrt{2}(2-(5/8)e^3\sqrt{2}-2\varepsilon)}{\pi(3-4e\sqrt{2}-e)}}, \ e = 0.339 \qquad (26)$$

Term β is employed to ensure that when PCM is solid, velocity remains equal to the initial value of zero. β and S are defined as in Eqs. 27 - 30, respectively:

$$\beta = \begin{cases} 0, & \text{if } T < \left(T_m - \frac{\Delta T_m}{2}\right) \\ \frac{T - \left(T_m - \frac{\Delta T_m}{2}\right)}{\Delta T_m}, & \text{if }\left(T_m - \frac{\Delta T_m}{2}\right) \leq T < \left(T_m + \frac{\Delta T_m}{2}\right) \\ 1, & \text{if } T > \left(T_m + \frac{\Delta T_m}{2}\right) \end{cases} \qquad (27)$$

$$S_u = A_{mush}\frac{(1-\beta)^2}{b_{mush}+\beta^3}u_f \qquad (28)$$

$$S_v = A_{mush}\frac{(1-\beta)^2}{b_{mush}+\beta^3}v_f \qquad (29)$$

$$S_w = A_{mush}\frac{(1-\beta)^2}{b_{mush}+\beta^3}w_f \qquad (30)$$

The two terms A_{mush} which denotes geometrical constant and b_{mush} which is used to avoid zero division and subtract from the Carmen-Kozney equation [20, 21]. In this study, we assumed $A_{mush} = 10^4$ while $b_{mush} = 10^{-3}$. The interfacial heat transfer coefficient h_{sf} and interfacial surface area a_{sf} are calculated based on Zhukauskas' correlations in Eqs. 31-32 [22]:

$$a_{sf} = \frac{3\pi d_f}{d_p^2} \qquad (31)$$

$$h_{sf} = Nu\frac{k_f}{d_f} \qquad (32)$$

The Nusselt number (Nu) is determined by the Eq. 33 correlation [23]:

$$Nu = \begin{cases} 0.76Re^{0.4}Pr^{0.37}, & \text{if } 0 < Re \leq 40 \\ 0.52Re^{0.5}Pr^{0.37}, & \text{if } 40 < Re \leq 1000 \\ 0.26Re^{0.6}Pr^{0.37}, & \text{if } 1000 < Re \leq 2\times10^5 \end{cases} \qquad (33)$$

The Re and Pr are non-dimensional variables calculated as in Eqs. 34-35:

$$Re = \frac{u_m\rho_f d_k}{\mu_f}, \ u_m = \sqrt{u_f^2 + v_f^2 + w_f^2} \qquad (34)$$

$$Pr = \frac{v_f}{\alpha_f}, \ v_f = \frac{\mu_f}{\rho_f} \qquad (35)$$

3. Results and Observations

3.1. Phase Change Materials and Metal Foam

Phase change materials retain thermal energy, allowing temperature stabilization for PVT collectors [24]. During the melting and freezing cycles, PCM undergoes a physical change that allows energy to be stored and released later as "latent" heat. However, given that the structure of paraffin as an organic hydrocarbon has a low thermal conductivity, a copper foam was used to retain the temperature gradients within the PVT collector [25]. Table 1 illustrates the thermophysical properties and other specifications of the utilized paraffin wax and copper foam.

Table 1. Thermophysical Properties of PCM and copper foam

Property	PCM	Copper Foam
Solid-state density (ρ_s, Kg/m3)	930	8960
Liquid-state density (ρ_f, Kg/m³)	830	-
Thermal conductivity-Solid(k_s,W/m°K)	0.21	400
Thermal conductivity-Liquid(k_f,W/m°K)	0.15	-
Latent heat of fusion (L_f, kJ/kg)	196	-
Dynamic viscosity (μ, Pa.s)	7.1×10^{-3}	-
Thermal expansion coefficient (α, 1/°K)	7.78×10^{-4}	-

Solid state-specific heat ($c_{p,s}$, J/kg˚K)	2100	385
Liquid state-specific heat ($c_{p,f}$, J/kg˚K)	2100	-
Melting point temperature (T_m, ˚C)	49	-
Melting range (ΔT_m, ˚C)	2	-
Porosity (ε, 1)	-	90%
Pores Per Inch (PPI) (ω, 1)	-	40

3.2. Verification

The simulation findings were validated by comparing them to an investigation by Browne et al. [26] and a simulation study by Mousavi et al. [27]. To this end, the mass flow rate, phase change material, and porous metal foam from both investigations were utilized as a source for the present simulation. In addition, the impacts of mass flow rates on thermal efficiency were compared with recent research results. Moreover, the mesh independence analysis has been done for the present modeling. The number of elements selected for the current study is 750640 in the case of PCM plus CFM presence. By further refinement of mesh, no significant change was discovered in fluid outlet temperature, hence the employed number of elements was sufficient.

3.3. Efficiency analysis

The thermal efficiency was computed using the Duffie and Beckman equation, as shown in Eq. 36 [28]:

$$\eta_{I,th} = \frac{Q_u}{G_{STC} \times A_c} \qquad (36)$$

η_{th}, G_{STC}, A_c and Q_u denote the thermal efficiency, solar irradiance under the standard test conditions, panel area, and effective heat collected. PVT collector's thermal efficiency is represented by Eq. 37:

$$Q_u = \dot{m} \times C_p \times (T_{out} - T_{in}) \qquad (37)$$

PVT collector's electrical efficiency is represented by Eq. 38:

$$\eta_{el} = \eta_{el,n} \times [1 - \beta_r(T_{panel} - 25°)] \qquad (38)$$

3.4. The Mass Flow Rate Effect

The mass flow rate is a crucial determinant of the thermal performance of PVT systems. Nevertheless, the optimum mass flow rate must be determined as low and high rates result in reduced efficiency and energy costs. Fig. 2 shows that as the mass flow rate increases, the thermal efficiency improves. The experiment results indicate that the optimum mass flow rate is about 0.01kg/s. Fig. 3 illustrates the influence of increasing mass flow rates on the electrical efficiency of the PVT collector whether PCM is employed alone or in

conjunction with a porous medium. As shown, the incorporation of PCM reduces PVT temperature by acting as thermal storage. During the phase change process, a fraction of solar radiation will be absorbed by melting PCM, hence dissipating the PVT temperature. During the melting process, the heat transfer rate from PVT to the PCM is reduced because of the formation of a thermally resistant interface. Therefore, implementing a metal foam will overcome the thermal resistance by lending higher conductivity. While using PCM caused higher thermal efficiency for the collector, using PCM incorporated with a porous medium resulted in higher electrical efficiency, as shown in Fig. 2 and Fig. 3. Fig. 4 indicates that the electrical efficiency decreases drastically as the average PV temperature increases [29]. In fact, for every 1-degree Celsius decrease in PVT temperature, the collector's electrical efficiency increases by about 0.06%.
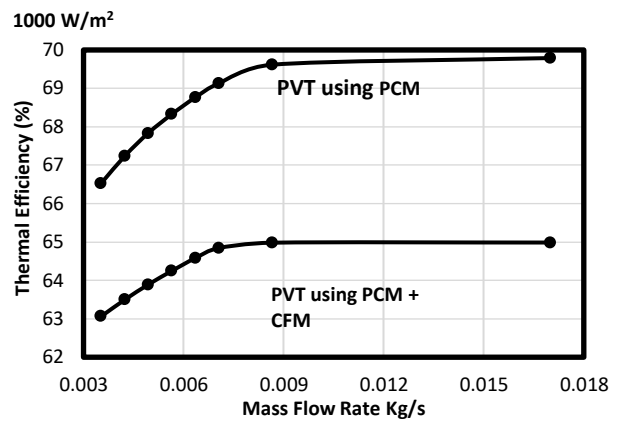

Fig. 2. Thermal efficiency of PVT using PCM and PCM Copper Foam for various mass flow rates
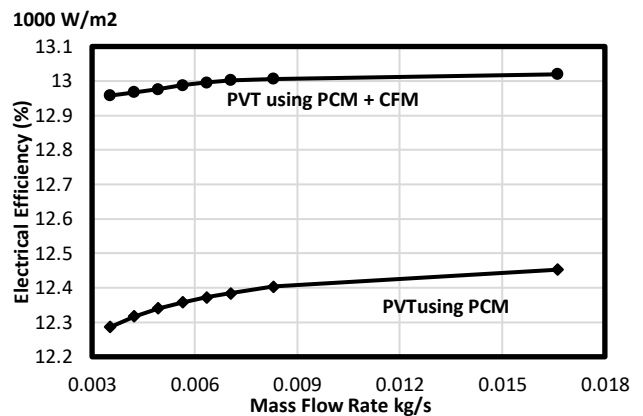

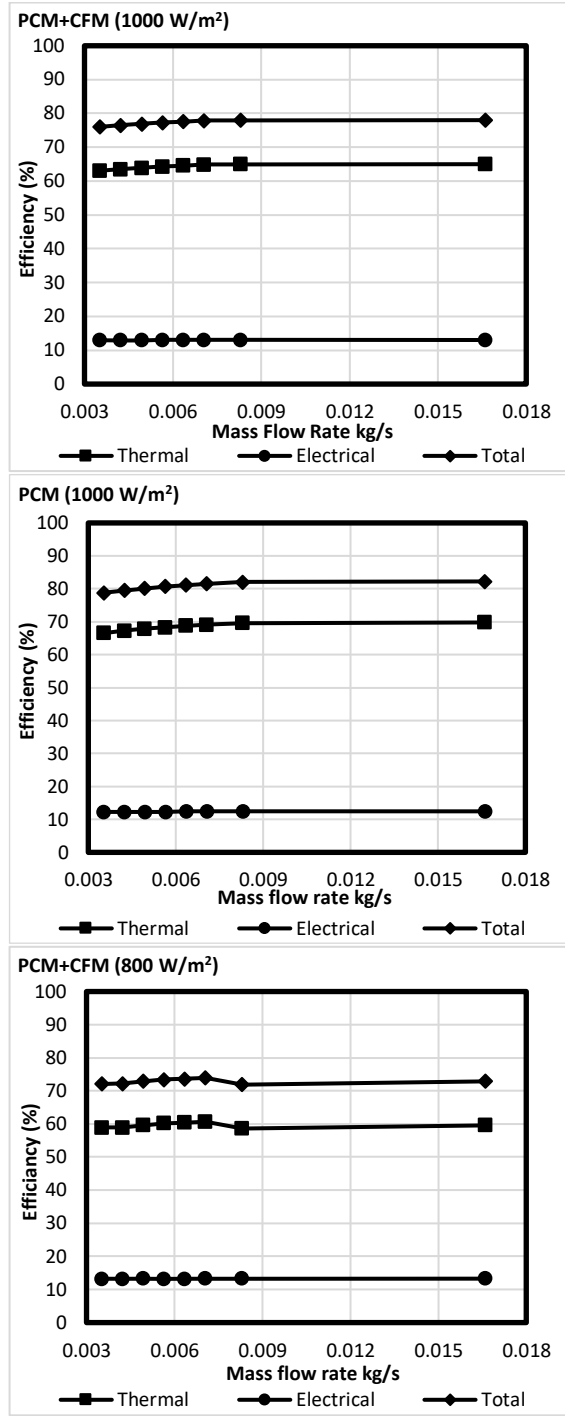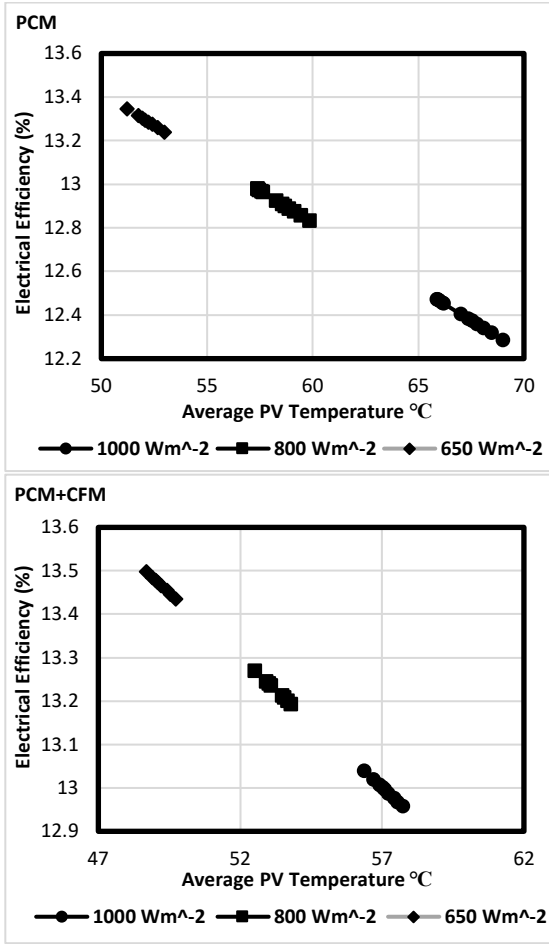**Fig. 3.** Electrical efficiency of PVT using PCM and PCM Copper Foam for various mass flow rates

Fig. 4. Effects of average PV temperature on electrical efficiency at different irradiance values with PCM alone and incorporated with CFM.

3.5. Optimizing Efficiency of PV/T

Thermal absorbers are important in optimizing integrated collectors' thermal and electrical performance by directly affecting PV modules' cooling [30]. The numerical analyses were carried out to test the effects of the thermal conductivity behaviour of PCM as a standalone and in combination with CFM on PVT efficiencies under three solar irradiance intensities. Fig. 5 summarize the analysis results by presenting the thermal, electrical, and total efficiencies. The cumulative energy performance of the designed collector was obtained by combining the thermal and electrical efficiency values. Solar irradiance of 1000 (W/m2) resulted in electrical efficiencies varying from 12.3 to 13.4%, while thermal efficiencies varied from 66.6 to 69.5% when PCM was present and from 63.5 to 65.5% when PCM and CFM were both presents. Even though the overall performance of the PVT in the presence of PCM was higher than that of PCM+CFM, the higher thermal efficiency was recorded at a higher average PV temperature (Fig. 6). The optimal configuration seems to rely on the overall efficiency and energy balance of the PVT collector. As appears in Fig. 5 the mass flow rate at which the maximum efficiencies were achieved was about 0.01kg/s.
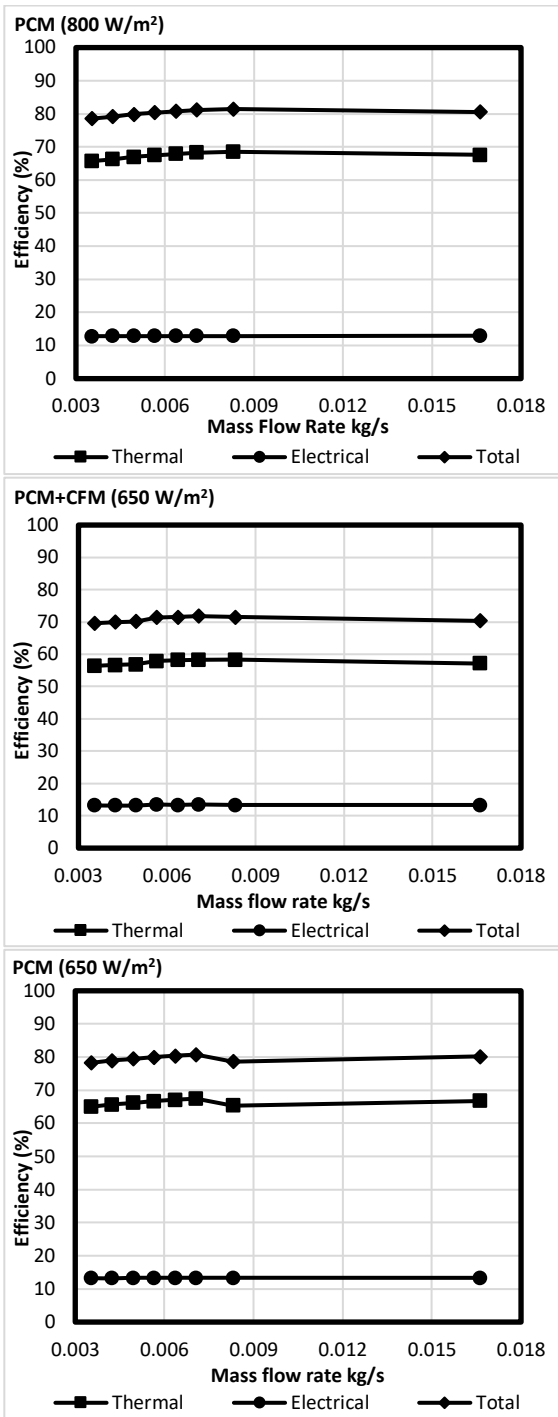
Fig. 6. comparison of thermal efficiency of the PVT systems under various irradiance regimes

3.6. Balancing PVT Energy Outputs

Thermal behaviour of cooling materials, ambient and coolant temperature, mass flow rate, PV and thermal module designs, and solar irradiance are just a few aspects that affect the PVT system's performance [31, 32]. Al-Waeli et al. reported that a 10°C rise in the temperature of the PV module might lead to a reduction in the photovoltaic efficiency to 5% [33]. The research acknowledged that the 1°C rise in the PV temperature would reduce the electrical efficiency to about 0.4 - 0.5% for the crystalline silicon cell. Fig. 7 shows that, in both cases, using PCM alone or with CFM, an increase in ΔT (water inlet and outlet temperature difference) strictly linked to solar radiation results in reduced thermal efficiencies. In the case of PCM coolant, the increase of 4°C resulted in a reduction in thermal efficiency of about 3.5%. At the same time, the same temperature increase in the PCM+CFM coolant was about 2% under the solar irradiation of 1000 (W/m2), indicating the latter coolant's heat absorbance, which positively affects the thermal efficiencies. On the other hand, the highest thermal efficiencies were obtained when the mass flow rates of coolants approached 0.01(kg/s), after which no increase was recorded.

Fig. 5. Thermal and electrical outputs of PV/T collector as functions of solar irradiances under PCM and PCM+CFM module cooling at different mass flow rates

Fig. 6 indicates that higher thermal efficiencies (69%) in the case of using PCM as a coolant under the 1000 (W/m2) irradiance regime may not be desirable given the higher average PV temperature (67 °C) that coincided because, the higher the PVT temperature, the lower the electrical efficiency gained. It is particularly emphasized when considering that 65% thermal efficiency was obtained at an average PV temperature of 57°C when using combined PCM+CFM as a coolant under the same irradiance intensity.
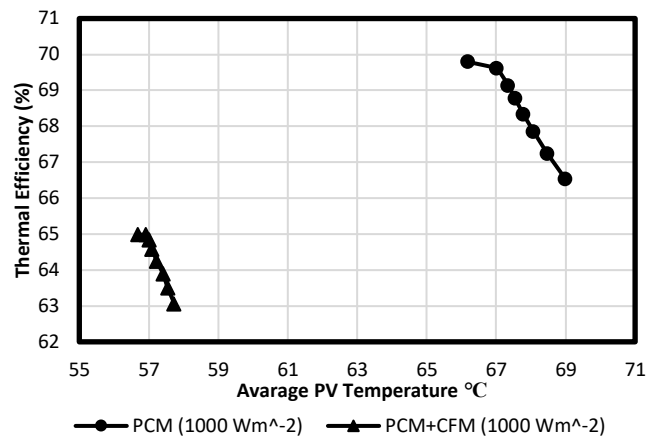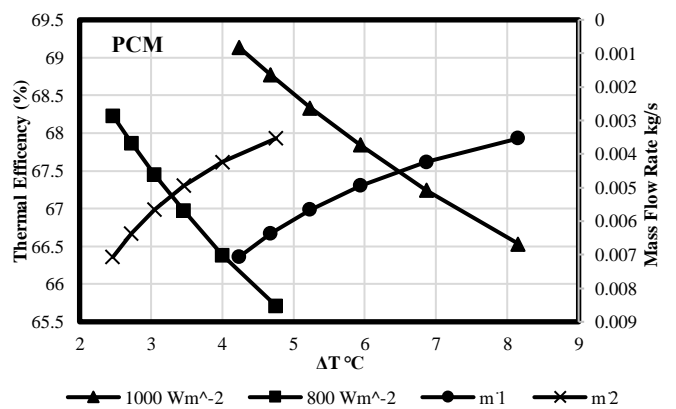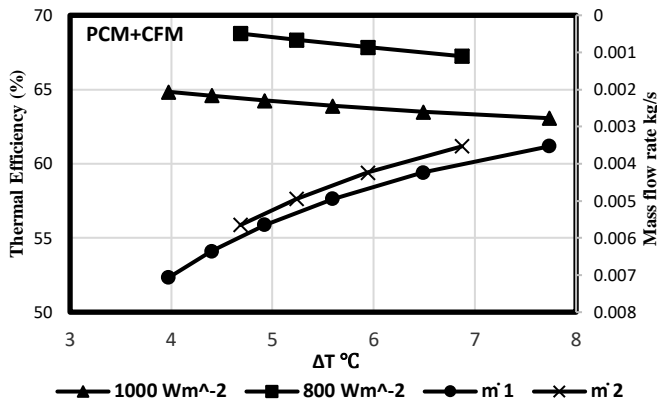
Fig. 7. Thermal efficiency as a function of mass flow rate and ΔT using PCM and PCM+CFM coolants under two solar irradiation regimes.

3.7. Exergy Analysis

The maximum amount of work possible from a system can be determined by calculating its exergy, as required by the second law of thermodynamics [34]. Therefore, thermal exergy was described according to Eq. 39-40:

$$T_b = \frac{T_{out} - T_{in}}{\ln\frac{T_{out}}{T_{in}}} \qquad (39)$$

$$\dot{E}_{x,th} = \dot{m}_f \times C_{P,f} \times (T_{out} - T_{in}) \times \left(1 - \frac{T_0}{T_b}\right) \qquad (40)$$

Furthermore, the equations for solar and electrical exergy are provided as Eqs. 41-42:

$$\dot{E}_{x,solar} = G \times A_c \times \left[1 - \frac{4}{3}\frac{T_0}{T_{sun}} + \frac{1}{3}\left(\frac{T_0}{T_{sun}}\right)^4\right] \qquad (41)$$

$$\dot{E}_{x,el} = \eta_{el} \times G \times A_c \qquad (42)$$

As previously stated, the second law efficiency may be derived using Eq. 43:

$$\eta_{II} = \frac{\dot{E}_{x,useful}}{\dot{E}_{x,solar}} = \frac{\dot{E}_{x,el} + \dot{E}_{x,th}}{\dot{E}_{x,solar}} \qquad (43)$$

By substituting these exergy terms, the second law efficiency equation can be rewritten as Eq. 44:

$$\eta_{II} = \frac{1}{\left[1 - \frac{4}{3}\frac{T_0}{T_{sun}} + \frac{1}{3}\left(\frac{T_0}{T_{sun}}\right)^4\right]}\left[\eta_{I,th}\left(1 - \frac{T_0}{T_b}\right) + \eta_{el}\right] \qquad (44)$$

Dead state conditions for computing exergy terms are 298.15 K and 100 kPa. As a blackbody, the sun was thought to have a temperature of 5774 K.

3.8. Exergy efficiency analysis

The exergy PVT with PCM is slightly lower than PVT with PCM plus porous copper foam. Using PCM+CFM, the electrical exergy has compensated for the decrease in thermal

exergy compared to the PVT using PCM (Fig. 8). Moreover, the exergy of the PVT utilizing a PCM-filled porous medium is much greater than that of the PCM-incorporated PVT, with an exergy efficiency of 14.4% under dead state conditions.
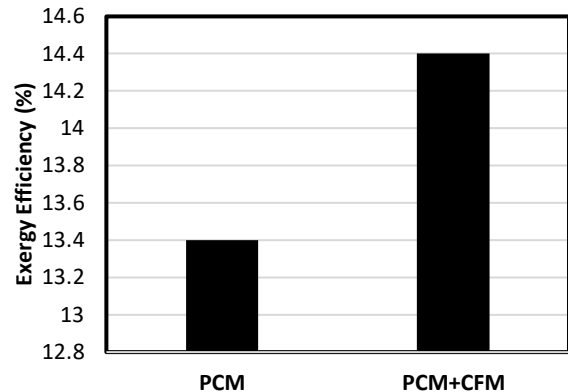

Fig. 8. Exergy efficiency influenced by implementation of standalone PCM or combined with CFM.

4. Conclusion

Numerical CFD modelling was utilized to investigate the effects of incorporating Phase Change Materials (PCMs) embedded in Copper Foam Matrix (CFM) on the enhancement of electrical efficiencies of the collector. The collector's thermal efficiency, including CFM, is lower than the conventional PCM due to the increment in temperature distribution that occurred in PCM. Additionally, our findings showed that the incorporation of CFM led to a 12% increase in the phase change of PCM, thanks to the higher effective conductivity of the CFM. This, in turn, resulted in increased heat storage in the PCM, which can be released at night when there is no sunlight available. Moreover, the total exergy efficiency of both collectors was calculated, and the proposed collector showed higher efficiency than the conventional. The proposed collector's most challenging factor is the CFM's high price. For this reason, further investigation into the use of porous media in solar energy would be an interesting topic for future work. Further research should be done in the field to increase the total efficiency of PVT and discover ways to reduce the cost of fabrication. As a potential solution, future research could investigate the use of other porous materials that could achieve similar results at a lower cost. In addition, modifications to the design or manufacturing process could potentially reduce the cost of using Copper Foam Matrix. These avenues of investigation would be interesting topics for future work in the field. It is important to note that any potential alternatives should also be evaluated in terms of their environmental impact and overall sustainability. By exploring these avenues, we can work towards developing more cost-effective and sustainable solutions for solar energy collection and storage.

Acknowledgements

References

[1] R. Daghigh, M. H. Ruslan, A. Zaharim, and K. Sopian, "Monthly performance of a photovoltaic thermal (PV/T) water heating system," 01/01 2011.

[2] M. Farshchimonfared, J. I. Bilbao, and A. B. Sproul, "Full optimisation and sensitivity analysis of a photovoltaic–thermal (PV/T) air system linked to a typical residential building," Solar Energy, vol. 136, pp. 15-22, 2016/10/15/ 2016, doi: 10.1016/j.solener.2016.06.048.

[3] X.-l. Meng, X.-l. Xia, C. Sun, Y. Li, and X.-l. Li, "A novel free-form Cassegrain concentrator for PV/T combining utilization," Solar Energy, vol. 135, pp. 864-873, 2016/10/01/ 2016, doi: 10.1016/j.solener.2016.06.034.

[4] F. Yazdanifard, E. Ebrahimnia-Bajestan, and M. Ameri, "Investigating the performance of a water-based photovoltaic/thermal (PV/T) collector in laminar and turbulent flow regime," Renewable Energy, vol. 99, pp. 295-306, 2016, doi: 10.1016/j.renene.2016.07.004.

[5] S. F. Jaber and A. M. Shakir, "Design and simulation of a boost-microinverter for optimized photovoltaic system performance," Int. J. SMART GRID (ijSmartGrid), vol. 5, no. 2, pp. 94-102, 2021.

[6] Y. Tripanagnostopoulos, M. Souliotis, R. Battisti, and A. Corrado, "Energy, cost and LCA results of PV and hybrid PV/T solar systems," Progress in Photovoltaics: Research and Applications, vol. 13, pp. 235-250, 05/01 2005, doi: 10.1002/pip.590.

[7] M. E. Shayan and G. Najafi, "Energy-economic optimization of thin layer photovoltaic on domes and cylindrical towers," International Journal of Smart Grid, vol. 3, no. 2, pp. 84-91, 2019.

[8] A. Harrouz, M. Abbes, I. Colak, and K. Kayisli, "Smart grid and renewable energy in Algeria," in 2017 IEEE 6th International Conference on Renewable Energy Research and Applications (ICRERA), 2017: IEEE, pp. 1166-1171.

[9] A. Hegazy, "Comparative study of performance of four photovoltaic/thermal solar air collectors," Energy Conversion and Management, vol. 41, pp. 861-881, 05/01 2000, doi: 10.1016/S0196-8904(99)00136-3.

[10] O. B. Kazanci, M. Skrupskelis, P. Sevela, G. K. Pavlov, and B. W. Olesen, "Sustainable heating, cooling and ventilation of a plus-energy house via photovoltaic/thermal panels," Energy and Buildings, vol. 83, pp. 122-129, 2014/11/01/ 2014, doi: 10.1016/j.enbuild.2013.12.064.

[11] Z. Qiu, X. Zhao, P. Li, X. Zhang, S. Ali, and J. Tan, "Theoretical investigation of the energy performance of a novel MPCM (Microencapsulated Phase Change Material) slurry based PV/T module," Energy, vol. 87, pp. 686-698, 2015/07/01/ 2015, doi: 10.1016/j.energy.2015.05.040.

[12] A. Hasan, S. J. McCormack, M. J. Huang, and B. Norton, "Energy and Cost Saving of a Photovoltaic-Phase Change Materials (PV-PCM) System through Temperature Regulation and Performance Enhancement of Photovoltaics," Energies, vol. 7, no. 3, pp. 1318-1331, 2014, doi: 10.3390/en7031318.

[13] M. Fiorentini, P. Cooper, and Z. Ma, "Development and optimization of an innovative HVAC system with integrated PVT and PCM thermal storage for a net-zero energy retrofitted house," Energy and Buildings, vol. 94, pp. 21-32, 2015/05/01/ 2015, doi: 10.1016/j.enbuild.2015.02.018.

[14] S. Kyaligonza and E. Cetkin, "Photovoltaic System Efficiency Enhancement with Thermal Management: Phase Changing Materials (PCM) with High Conductivity Inserts," Int. J. Smart grid, vol. 5, no. 4, pp. 138-148, 2021.

[15] Y. B. Tao, Y. You, and Y. L. He, "Lattice Boltzmann simulation on phase change heat transfer in metal foams/paraffin composite phase change material," Applied Thermal Engineering, vol. 93, pp. 476-485, 2016/01/25/ 2016, doi: 10.1016/j.applthermaleng.2015.10.016.

[16] D. Zhou and C. Y. Zhao, "Experimental investigations on heat transfer in phase change materials (PCMs) embedded in porous materials," Applied Thermal Engineering, vol. 31, no. 5, pp. 970-977, 2011/04/01/ 2011, doi: 10.1016/j.applthermaleng.2010.11.022.

[17] Y. Du and Y. Ding, "Towards improving charge/discharge rate of latent heat thermal energy storage (LHTES) by embedding metal foams in phase change materials (PCMs)," Chemical Engineering and Processing: Process Intensification, vol. 108, pp. 181-188, 2016/10/01/ 2016, doi: 10.1016/j.cep.2016.08.003.

[18] G. Hwang, C. Wu, and C.-H. Chao, "Investigation of Non-Darcian Forced Convection in an Asymmetrically Heated Sintered Porous Channel," Journal of Heat Transfer-transactions of The Asme - J HEAT TRANSFER, vol. 117, pp. 725-732, 08/01 1995, doi: 10.1115/1.2822636.

[19] K. Boomsma and D. Poulikakos, "Corrigendum for the paper: K. Boomsma, D. Poulikakos, "On the effective thermal conductivity of a three-dimensionally structured fluid-saturated metal foam" [International Journal of Heat and Mass Transfer, 44 (2001) 827–836]," International Journal of Heat and Mass Transfer, vol. 54, no. 1, pp. 746-748, 2011/01/15/ 2011, doi: 10.1016/j.ijheatmasstransfer.2010.08.023.

[20] Y. Hong, W.-B. Ye, J. Du, and S.-M. Huang, "Solid-liquid phase-change thermal storage and release behaviors in a rectangular cavity under the impacts of mushy region and low gravity," International Journal of Heat and Mass Transfer, vol. 130, pp. 1120-1132, 2019/03/01/ 2019, doi: 10.1016/j.ijheatmasstransfer.2018.11.024.

[21] M. Fadl and P. C. Eames, "Numerical investigation of the influence of mushy zone parameter Amush on heat transfer characteristics in vertically and horizontally oriented thermal energy storage systems," Applied Thermal

Engineering, vol. 151, pp. 90-99, 2019/03/25/ 2019, doi: 10.1016/j.applthermaleng.2019.01.102.

[22] A. Žukauskas, "Heat Transfer from Tubes in Crossflow," in Advances in Heat Transfer, vol. 8, J. P. Hartnett and T. F. Irvine Eds.: Elsevier, 1972, pp. 93-160.

[23] X. Zhang, G. Su, J. Lin, A. Liu, C. Wang, and Y. Zhuang, "Three-dimensional numerical investigation on melting performance of phase change material composited with copper foam in local thermal non-equilibrium containing an internal heater," International Journal of Heat and Mass Transfer, vol. 170, p. 121021, 2021/05/01/ 2021, doi: 10.1016/j.ijheatmasstransfer.2021.121021.

[24] A. Al-Waeli, K. Sopian, A. Ibrahim, M. Sohif, and M. H. Ruslan, "Concepts and Challenges of Nanofluids and Phase Change Material (PCM) in Photovoltaic Thermal (PV/T) Collectors: A Review," 09/24 2018, doi: 10.17576/jkukm-2018-SI-1(3).

[25] A. M. Abdulateef, J. Abdulateef, K. Sopian, S. Mat, and A. Ibrahim, "Optimal fin parameters used for enhancing the melting and solidification of phase-change material in a heat exchanger unite," Case Studies in Thermal Engineering, vol. 14, p. 100487, 2019/09/01/ 2019, doi: 10.1016/j.csite.2019.100487.

[26] M. C. Browne, B. Norton, and S. J. McCormack, "Heat retention of a photovoltaic/thermal collector with PCM," Solar Energy, vol. 133, pp. 533-548, 2016/08/01/ 2016, doi: 10.1016/j.solener.2016.04.024.

[27] S. Mousavi, A. Kasaeian, M. B. Shafii, and M. H. Jahangir, "Numerical investigation of the effects of a copper foam filled with phase change materials in a water-cooled photovoltaic/thermal system," Energy Conversion and Management, vol. 163, pp. 187-195, 2018/05/01/ 2018, doi: 10.1016/j.enconman.2018.02.039.

[28] J. A. Duffie and W. A. Beckman, Solar Engineering of Thermal Processes. Wiley, 1980.

[29] F. Javed and A. Raza, "Impact of Temperature & Illumination for Improvement in Photovoltaic System Efficiency," International Journal of Smart Grid, DOI, vol. 10, pp. 23-28, 2022.

[30] E. Ahmad et al., "Recent advances in passive cooling methods for photovoltaic performance enhancement," International Journal of Electrical and Computer Engineering, vol. 11, pp. 146-154, 02/01 2021, doi: 10.11591/ijece.v11i1.pp146-154.

[31] E. Ahmad, K. Sopian, A. Ibrahim, C. Gan, and S. Razak, "Experimental investigation of passively cooled photovoltaic modules on the power output performance," International Journal of Power Electronics and Drive Systems, vol. 13, pp. 520-527, 03/01 2022, doi: 10.11591/ijpeds.v13.i1.pp520-527.

[32] R. K. Ajeel, R. Zulkifli, K. Sopian, S. N. Fayyadh, A. Fazlizan, and A. Ibrahim, "Numerical investigation of binary hybrid nanofluid in new configurations for curved-corrugated channel by thermal-hydraulic performance method," Powder Technology, vol. 385, pp. 144-159, 2021/06/01/ 2021, doi: 10.1016/j.powtec.2021.02.055.

[33] A. H. A. Al-Waeli, K. Sopian, H. A. Kazem, and M. T. Chaichan, "Photovoltaic/Thermal (PV/T) systems: Status and future prospects," Renewable and Sustainable Energy Reviews, vol. 77, pp. 109-130, 2017, doi: 10.1016/j.rser.2017.03.126.

[34] R. Saidur, G. BoroumandJazi, S. Mekhlif, and M. Jameel, "Exergy analysis of solar energy applications," Renewable and Sustainable Energy Reviews, vol. 16, no. 1, pp. 350-356, 2012/01/01/ 2012, doi: 10.1016/j.rser.2011.07.162.